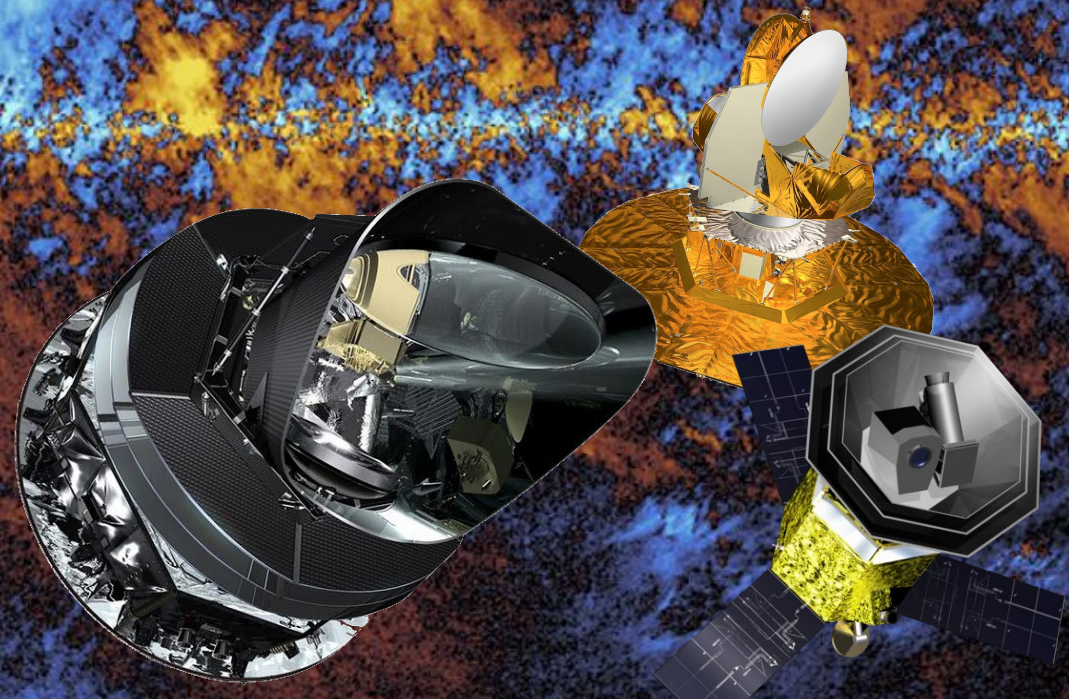


Intensity foregrounds and priors

Kristian Joten Andersen



BeyondPlanck online release conference, November 18-20, 2020

The BeyondPlanck data model

$$d_{j,t} = g_{j,t} P_{tp,j} \left[\mathbf{B}_{pp',j}^{\text{symm}} \sum_c M_{c,j}(\beta_{p'}, \Delta_{\text{bp}}^j) a_{p'}^c + \mathbf{B}_{j,t}^{\text{asymm}} (s_j^{\text{orb}} + s_t^{\text{fsl}}) \right] + n_{j,t}^{\text{corr}} + n_{j,t}^{\text{w}}$$

$$\begin{aligned} \mathbf{g} &\leftarrow P(\mathbf{g} \mid \mathbf{d}, \xi_n, \Delta_{\text{bp}}, \mathbf{a}, \beta, C_\ell) \\ \mathbf{n}_{\text{corr}} &\leftarrow P(\mathbf{n}_{\text{corr}} \mid \mathbf{d}, \mathbf{g}, \xi_n, \Delta_{\text{bp}}, \mathbf{a}, \beta, C_\ell) \\ \xi_n &\leftarrow P(\xi_n \mid \mathbf{d}, \mathbf{g}, \mathbf{n}_{\text{corr}}, \Delta_{\text{bp}}, \mathbf{a}, \beta, C_\ell) \\ \Delta_{\text{bp}} &\leftarrow P(\Delta_{\text{bp}} \mid \mathbf{d}, \mathbf{g}, \mathbf{n}_{\text{corr}}, \xi_n, \mathbf{a}, \beta, C_\ell) \\ \beta &\leftarrow P(\beta \mid \mathbf{d}, \mathbf{g}, \mathbf{n}_{\text{corr}}, \xi_n, \Delta_{\text{bp}}, C_\ell) \\ \mathbf{a} &\leftarrow P(\mathbf{a} \mid \mathbf{d}, \mathbf{g}, \mathbf{n}_{\text{corr}}, \xi_n, \Delta_{\text{bp}}, \beta, C_\ell) \\ C_\ell &\leftarrow P(C_\ell \mid \mathbf{d}, \mathbf{g}, \mathbf{n}_{\text{corr}}, \xi_n, \Delta_{\text{bp}}, \mathbf{a}, \beta) \end{aligned}$$

$$P(\mathbf{a}, \beta \mid \mathbf{d}, \mathbf{g}, \dots) = P(\mathbf{a}, \beta \mid \mathbf{d}) \quad \text{for simpler notation}$$

Bayes' theorem:

$$P(\mathbf{a}, \beta \mid \mathbf{d}) = \frac{P(\mathbf{d} \mid \mathbf{a}, \beta)P(\mathbf{a}, \beta)}{P(\mathbf{d})} \propto \mathcal{L}(\mathbf{a}, \beta)P(\mathbf{a}, \beta)$$

Likelihood function

Priors

We'll get to these later

Gibbs sampling:

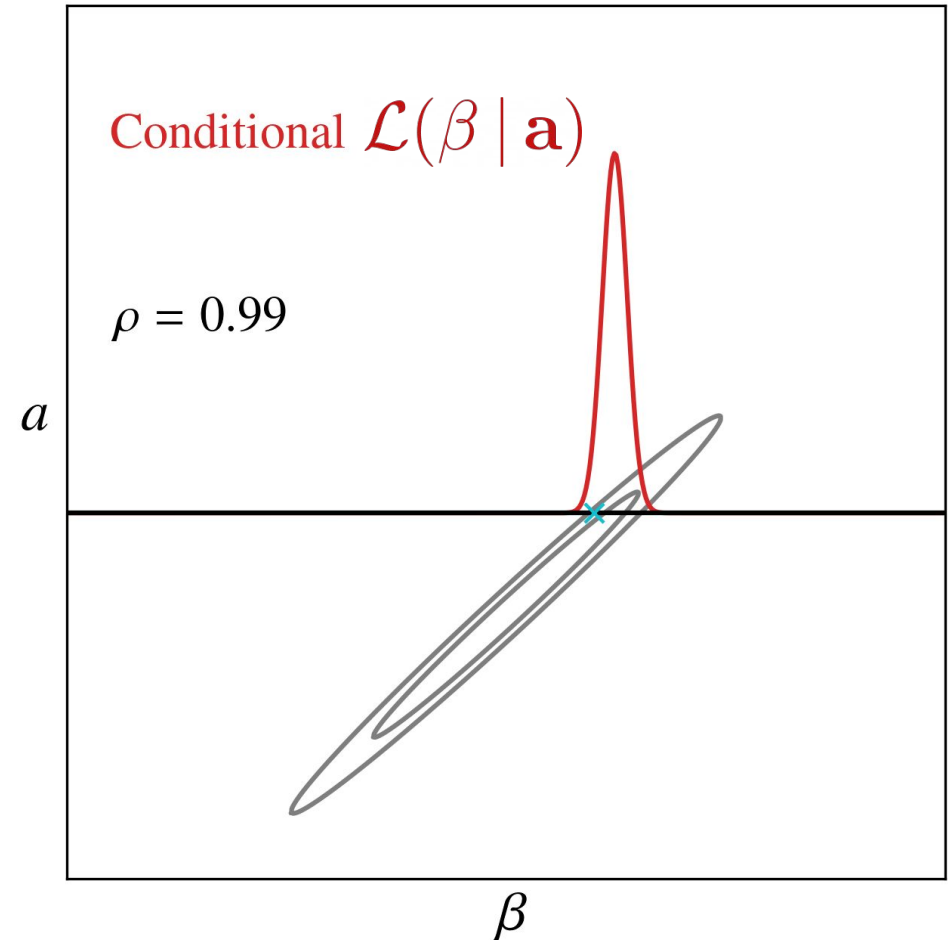
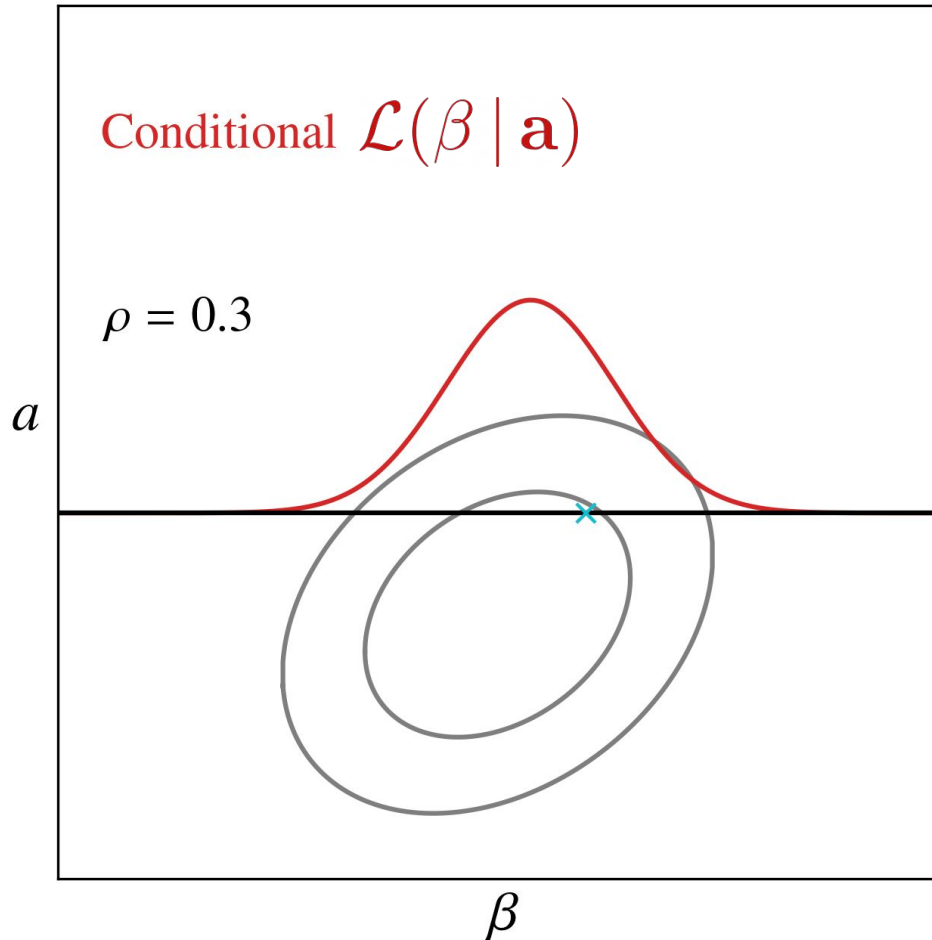
$$\beta \leftarrow P(\beta \mid \mathbf{d}, \mathbf{a}, \dots) \propto \mathcal{L}(\beta \mid \mathbf{a})P(\beta \mid \mathbf{a})$$

$$\mathbf{a} \leftarrow P(\mathbf{a} \mid \mathbf{d}, \beta, \dots) \propto \mathcal{L}(\mathbf{a} \mid \beta)P(\mathbf{a} \mid \beta)$$

The posterior distribution



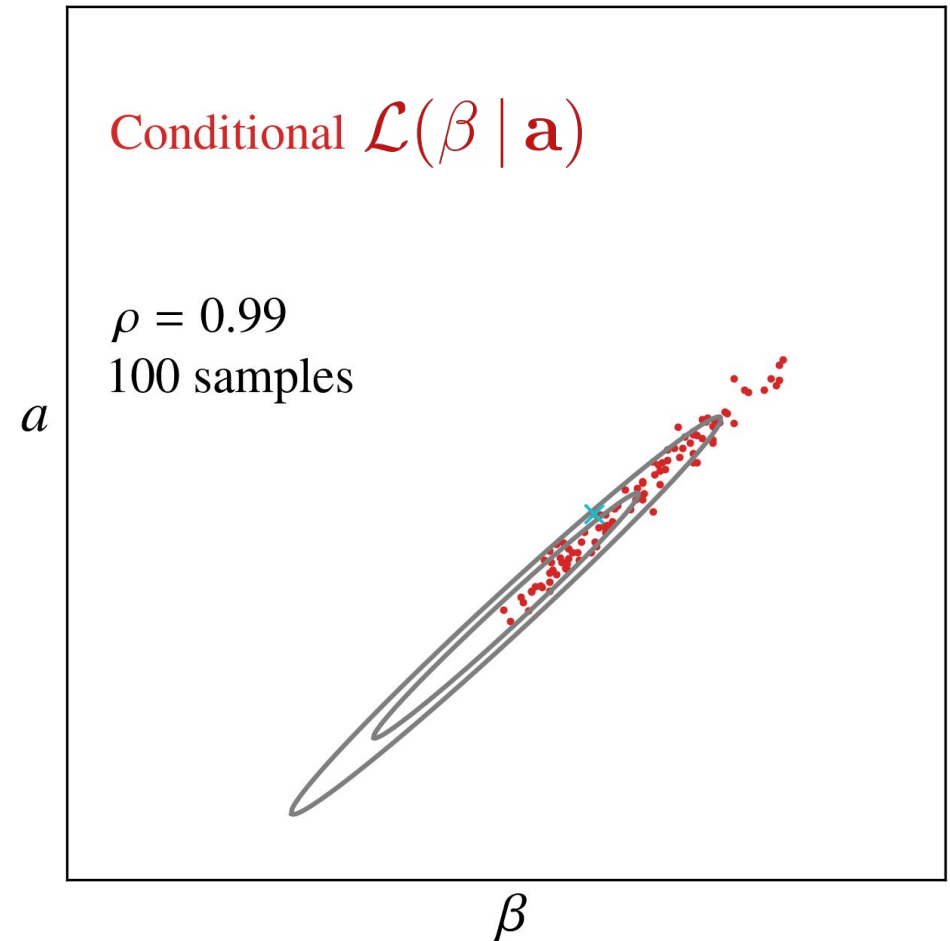
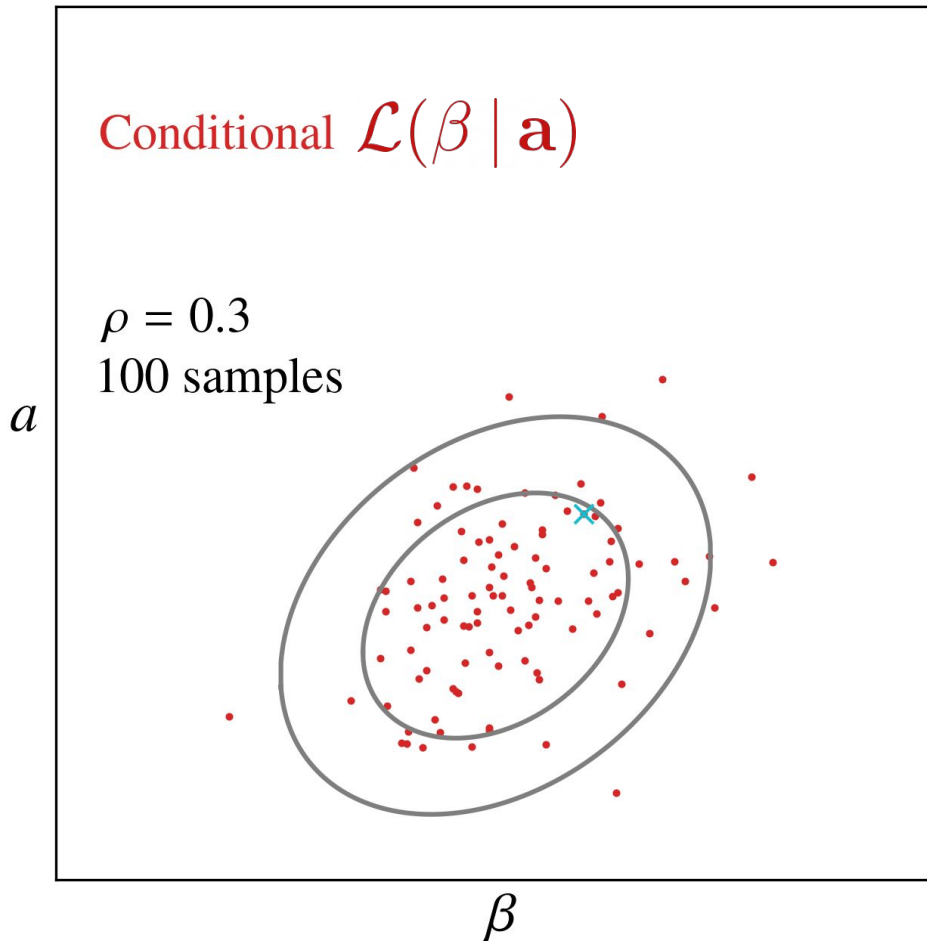
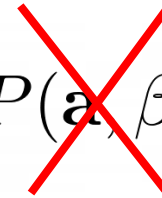
$$P(\mathbf{a}, \beta | \mathbf{d}) = \frac{P(\mathbf{d} | \mathbf{a}, \beta)P(\mathbf{a}, \beta)}{P(\mathbf{d})} \propto \mathcal{L}(\mathbf{a}, \beta)P(\mathbf{a}, \beta)$$



The posterior distribution



$$P(\mathbf{a}, \beta | \mathbf{d}) = \frac{P(\mathbf{d} | \mathbf{a}, \beta)P(\mathbf{a}, \beta)}{P(\mathbf{d})} \propto \mathcal{L}(\mathbf{a}, \beta)P(\mathbf{a}, \beta)$$



The posterior distribution



$$P(\mathbf{a}, \beta | \mathbf{d}) = \frac{P(\mathbf{d} | \mathbf{a}, \beta)P(\mathbf{a}, \beta)}{P(\mathbf{d})} \propto \mathcal{L}(\mathbf{a}, \beta)P(\mathbf{a}, \beta)$$

Likelihood function

$$\mathcal{L}(\mathbf{a}, \beta) = \mathcal{L}(\mathbf{a} | \beta)\mathcal{L}(\beta)$$

$$\beta \leftarrow \mathcal{L}(\beta)$$

$$\mathbf{a} \leftarrow \mathcal{L}(\mathbf{a} | \beta)$$

↑
Joint

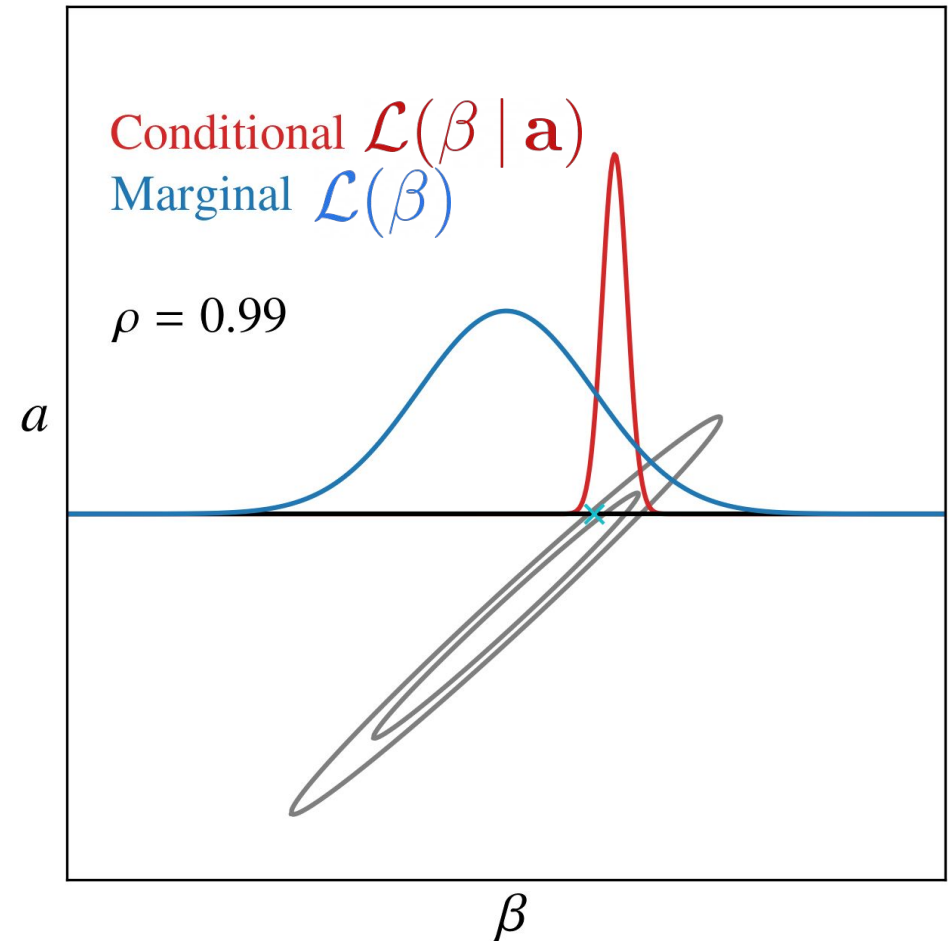
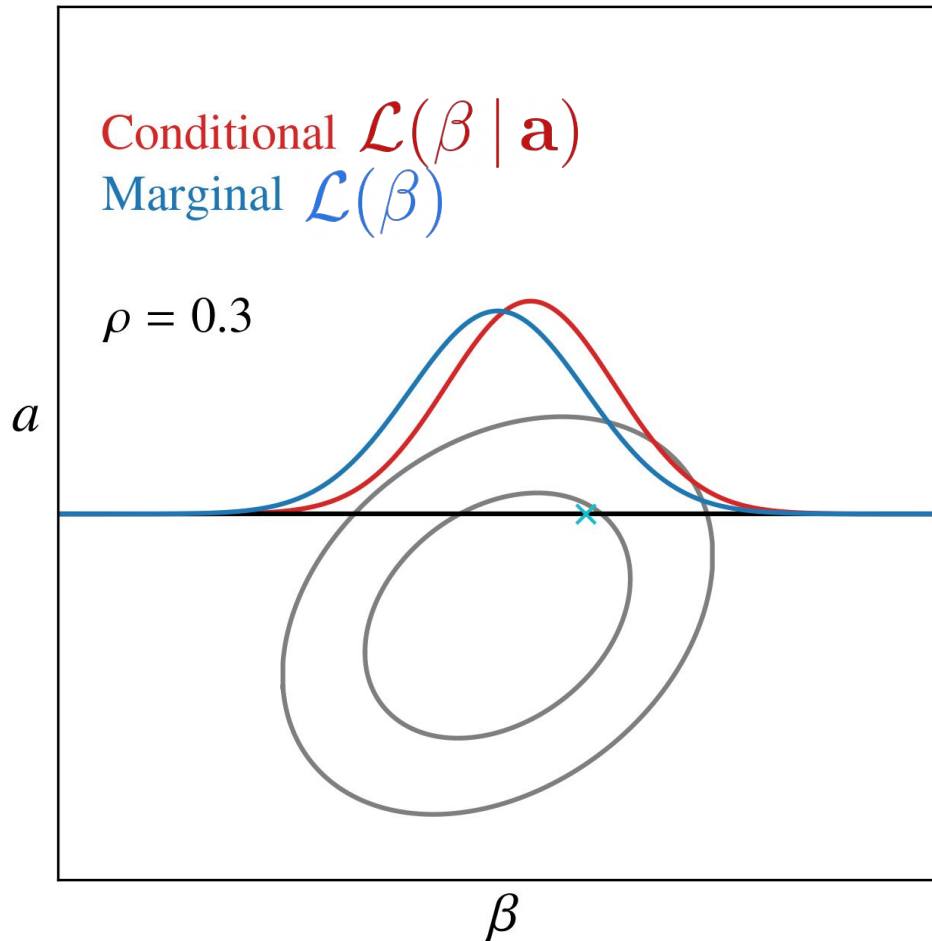
↑
Conditional

↑
Marginal

The posterior distribution



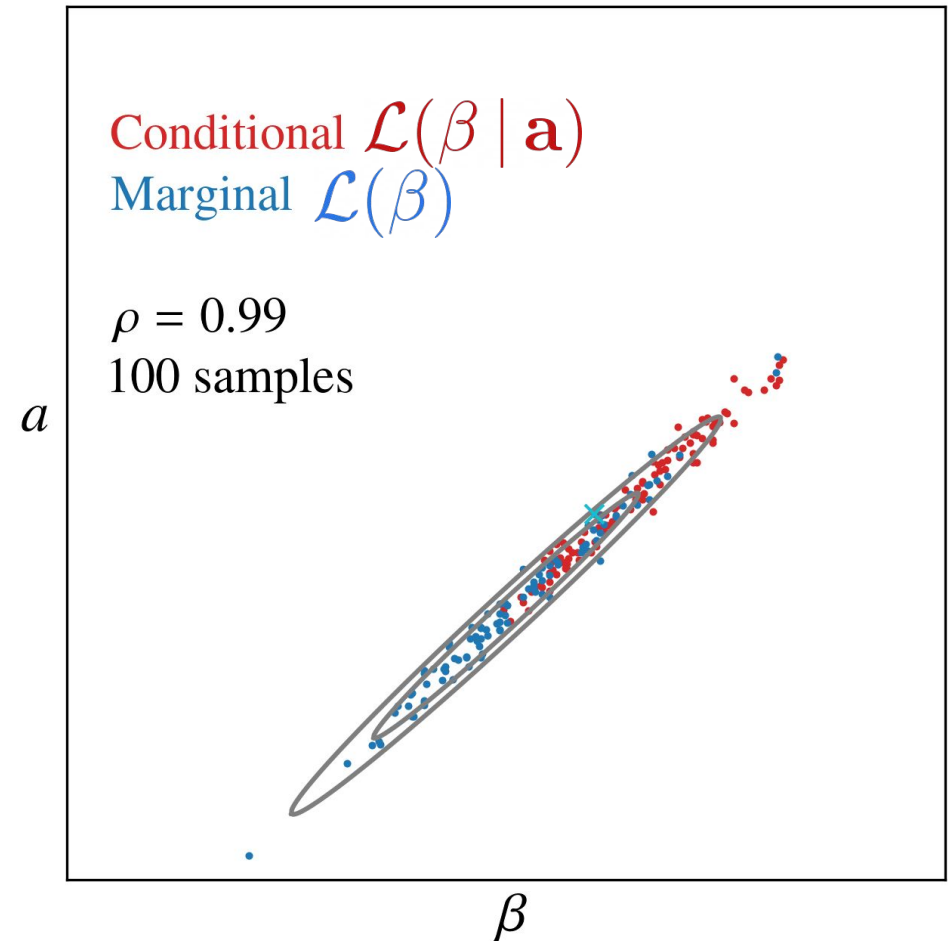
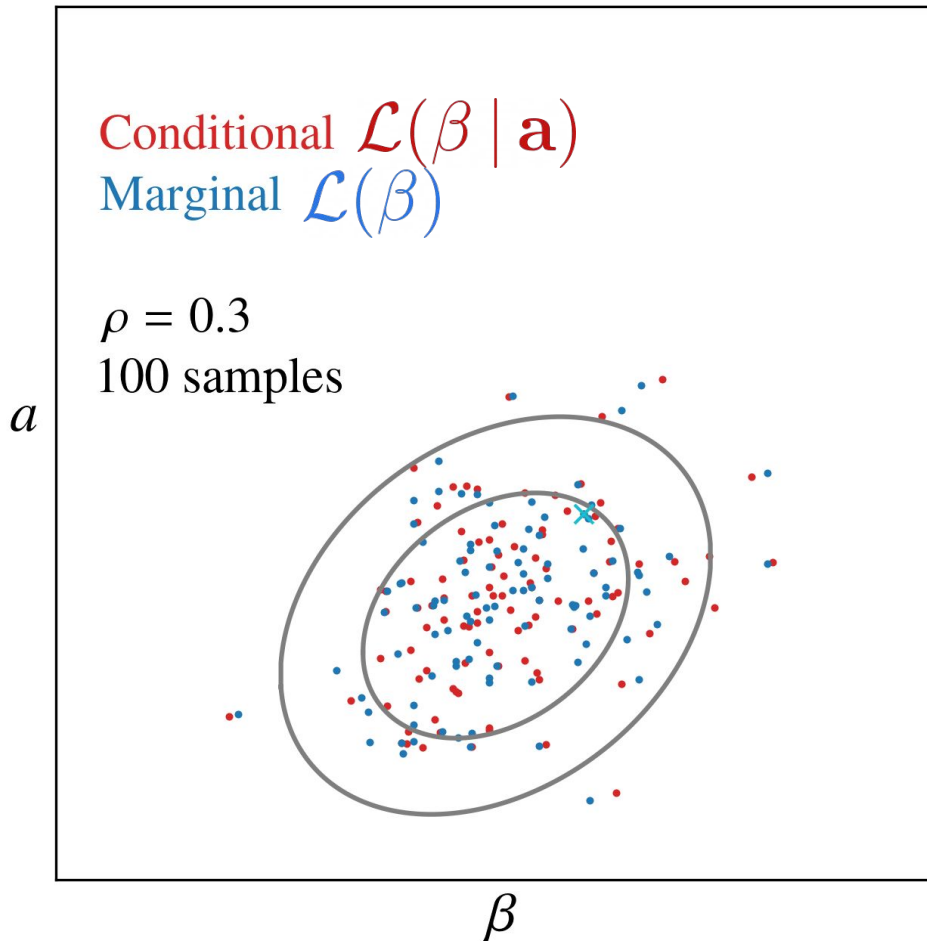
$$P(\mathbf{a}, \beta | \mathbf{d}) = \frac{P(\mathbf{d} | \mathbf{a}, \beta)P(\mathbf{a}, \beta)}{P(\mathbf{d})} \propto \mathcal{L}(\mathbf{a}, \beta)P(\mathbf{a}, \beta)$$



The posterior distribution



$$P(\mathbf{a}, \beta | \mathbf{d}) = \frac{P(\mathbf{d} | \mathbf{a}, \beta)P(\mathbf{a}, \beta)}{P(\mathbf{d})} \propto \mathcal{L}(\mathbf{a}, \beta)P(\mathbf{a}, \beta)$$



Conditional vs. marginal likelihood function

$$\mathcal{L}(\mathbf{a}, \beta) \propto \frac{e^{-\frac{1}{2}(\mathbf{m}_v - \mathbf{A}_v \mathbf{a})^T \mathbf{N}_v^{-1} (\mathbf{m}_v - \mathbf{A}_v \mathbf{a})}}{\sqrt{|2\pi \mathbf{N}_v^{-1}|}} \quad \text{assuming gaussian white noise}$$

$$-2 \ln \mathcal{L}(\mathbf{a}, \beta) = \text{const} + (\mathbf{m}_v - \mathbf{A}_v \mathbf{a})^T \mathbf{N}_v^{-1} (\mathbf{m}_v - \mathbf{A}_v \mathbf{a}) = \text{const} + \chi^2$$

Assume for computational efficiency:

- β varies more slowly than \mathbf{a}
- uniform pixelization and angular resolution for all \mathbf{m}_v
- \mathbf{N}_v is diagonal

Stompor et al. (2009, MNRAS, 392, 216) shows that per pixel (across all frequencies) the log-likelihood becomes

$$-2 \ln \mathcal{L}_{\text{ridge}}(\beta) = \text{const} + (\mathbf{A}^T \mathbf{N}^{-1} \mathbf{m})^T (\mathbf{A}^T \mathbf{N}^{-1} \mathbf{A})^{-1} (\mathbf{A}^T \mathbf{N}^{-1} \mathbf{m}),$$

$$\begin{aligned} -2 \ln \mathcal{L}_{\text{marg}}(\beta) &= -2 \ln \int d\mathbf{a} \exp \left[-\frac{1}{2} (\mathbf{m} - \mathbf{A}\mathbf{a})^T \mathbf{N}^{-1} (\mathbf{m} - \mathbf{A}\mathbf{a}) \right] \\ &= \text{const} + (\mathbf{A}^T \mathbf{N}^{-1} \mathbf{m})^T (\mathbf{A}^T \mathbf{N}^{-1} \mathbf{A})^{-1} (\mathbf{A}^T \mathbf{N}^{-1} \mathbf{m}) \\ &\quad + \ln |(\mathbf{A}^T \mathbf{N}^{-1} \mathbf{A})^{-1}|, \end{aligned}$$

Data model and priors

Free parameters

$$\begin{aligned}
 s_{\text{RJ}} = & \left(a_{\text{CMB}} + a_{\text{quad}}(\nu) \right) \frac{x^2 e^x}{(e^x - 1)^2} + \\
 & + a_s \left(\frac{\nu}{\nu_{0,s}} \right)^{\beta_s} + \\
 & + a_{\text{ff}} \left(\frac{\nu_{0,\text{ff}}}{\nu} \right)^2 \frac{g_{\text{ff}}(\nu; T_e)}{g_{\text{ff}}(\nu_{0,\text{ff}}; T_e)} + \\
 & + a_{\text{sd}} \left(\frac{\nu_{0,\text{sd}}}{\nu} \right)^2 \frac{f_{\text{sd}} \left(\nu \cdot \frac{\nu_p}{30.0 \text{ GHz}} \right)}{f_{\text{sd}} \left(\nu_{0,\text{sd}} \cdot \frac{\nu_p}{30.0 \text{ GHz}} \right)} + \\
 & + a_d \left(\frac{\nu}{\nu_{0,d}} \right)^{\beta_d + 1} \frac{e^{h\nu_{0,d}/k_B T_d} - 1}{e^{h\nu/k_B T_d} - 1} + \\
 & + \sum_{j=1}^{N_{\text{src}}} a_{j,\text{src}} \left(\frac{\nu}{\nu_{0,\text{src}}} \right)^{\alpha_{j,\text{src}} - 2},
 \end{aligned}$$

CMB

Synchrotron

Free-free

AME / Spinning dust

Thermal dust

Point sources

Not: Sunyaev-Zeldovich effect, zodiacal light, cosmic infrared background

Free parameters

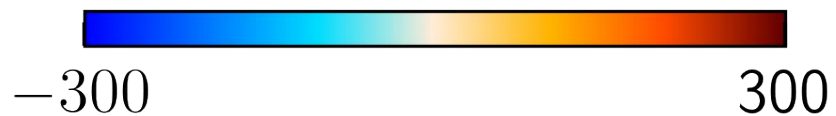
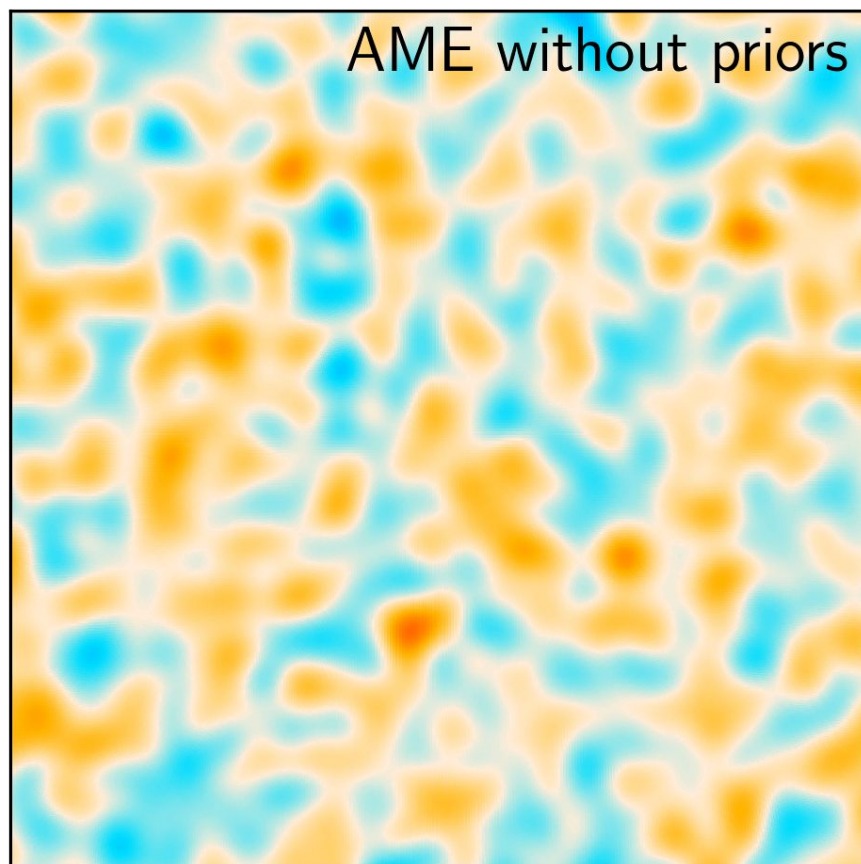
$$\begin{aligned}
 S_{\text{RJ}} = & \left(a_{\text{CMB}} + a_{\text{quad}}(\nu) \right) \frac{x^2 e^x}{(e^x - 1)^2} + \\
 & + a_s \left(\frac{\nu}{\nu_{0,s}} \right)^{\beta_s} + \\
 & + a_{\text{ff}} \left(\frac{\nu_{0,\text{ff}}}{\nu} \right)^2 \frac{g_{\text{ff}}(\nu; T_e)}{g_{\text{ff}}(\nu_{0,\text{ff}}; T_e)} + \\
 & + a_{\text{sd}} \left(\frac{\nu_{0,\text{sd}}}{\nu} \right)^2 \frac{f_{\text{sd}} \left(\nu \cdot \frac{\nu_p}{30.0 \text{ GHz}} \right)}{f_{\text{sd}} \left(\nu_{0,\text{sd}} \cdot \frac{\nu_p}{30.0 \text{ GHz}} \right)} + \\
 & + a_d \left(\frac{\nu}{\nu_{0,d}} \right)^{\beta_d + 1} \frac{e^{h\nu_{0,d}/k_B T_d} - 1}{e^{h\nu/k_B T_d} - 1} + \\
 & + \sum_{j=1}^{N_{\text{src}}} a_{j,\text{src}} \left(\frac{\nu}{\nu_{0,\text{src}}} \right)^{\alpha_{j,\text{src}} - 2},
 \end{aligned}$$

- Only the following data are included in the component separation analysis:
 - **Planck LFI 30, 44 and 70 GHz pixel maps, binned from time-ordered data** (Suur-Uski et al.2020)
 - **Planck 857 GHz** to constrain thermal dust intensity
 - **WMAP 33-61 GHz** to constrain low-frequency foregrounds
 - **Haslam 408 MHz** to constrain synchrotron intensity
- Intermediate *Planck HFI* and *WMAP 23 GHz* data are **not** included, because they have similar or higher signal-to-noise ratios than *Planck LFI*, which we want to be the **dominant** statistical driver.

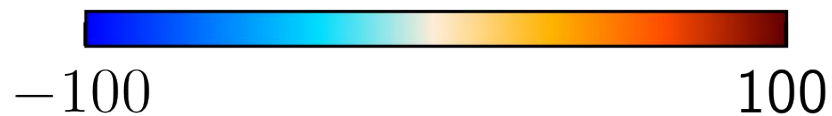
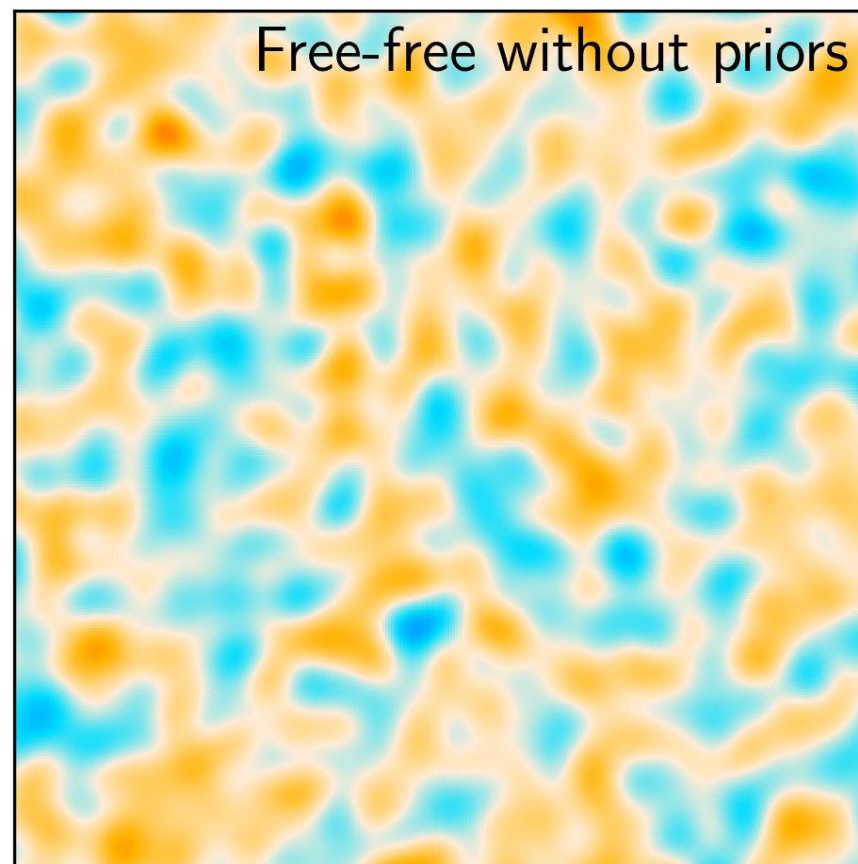
Amplitude degeneracies and priors



60' FWHM, $20^\circ \times 20^\circ$ centered on galactic south pole



μK_{RJ} at 22 GHz

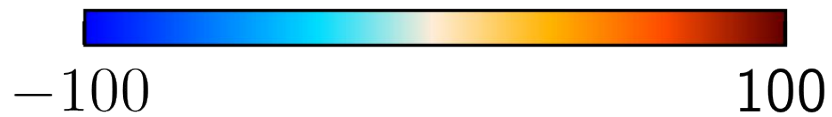
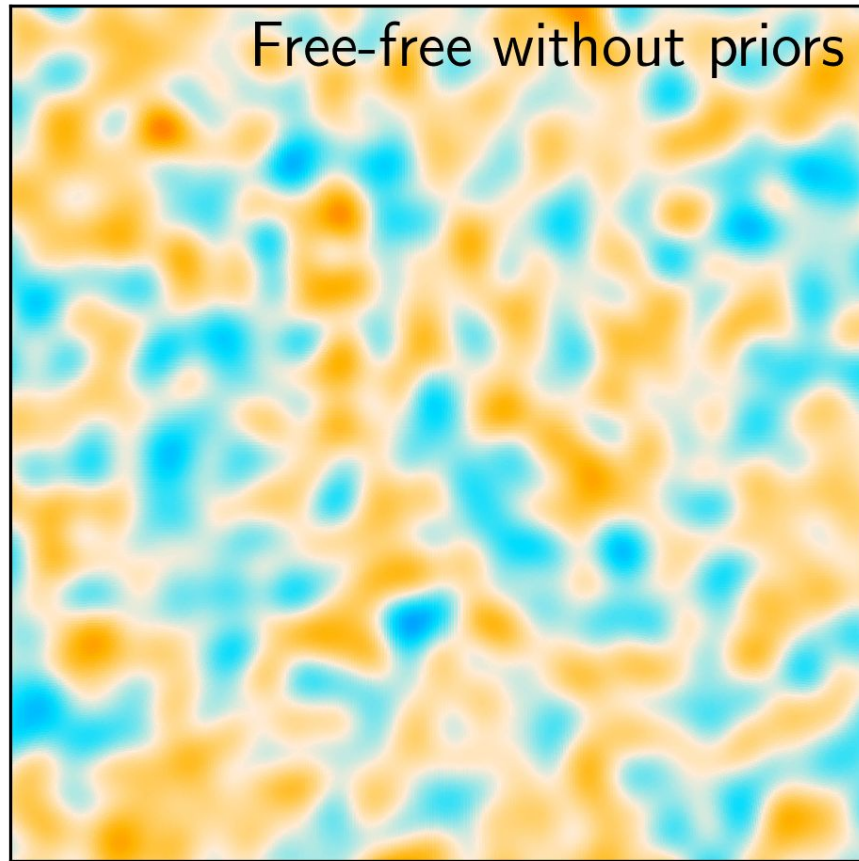


μK_{RJ} at 40 GHz

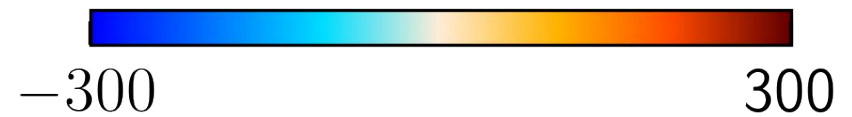
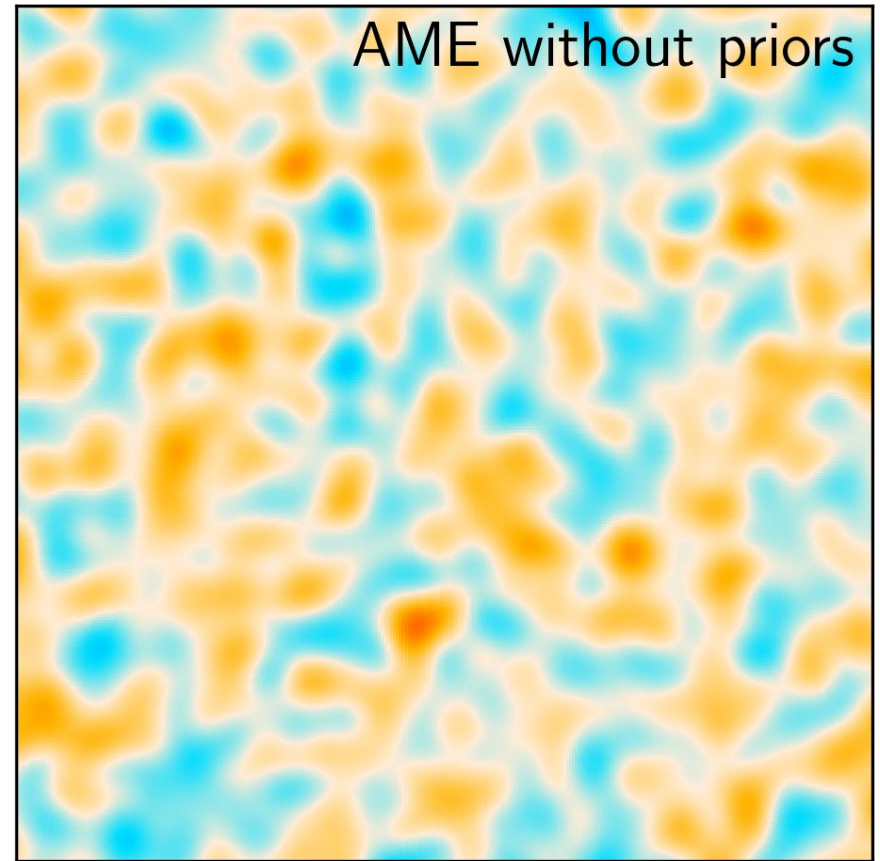
Amplitude degeneracies and priors



60' FWHM, $20^\circ \times 20^\circ$ centered on galactic south pole



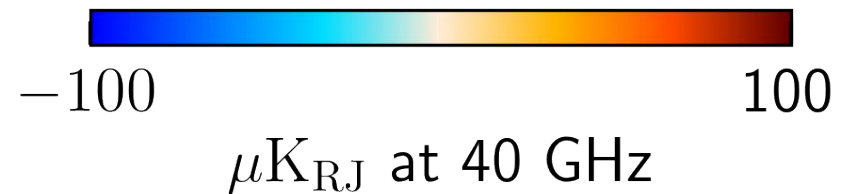
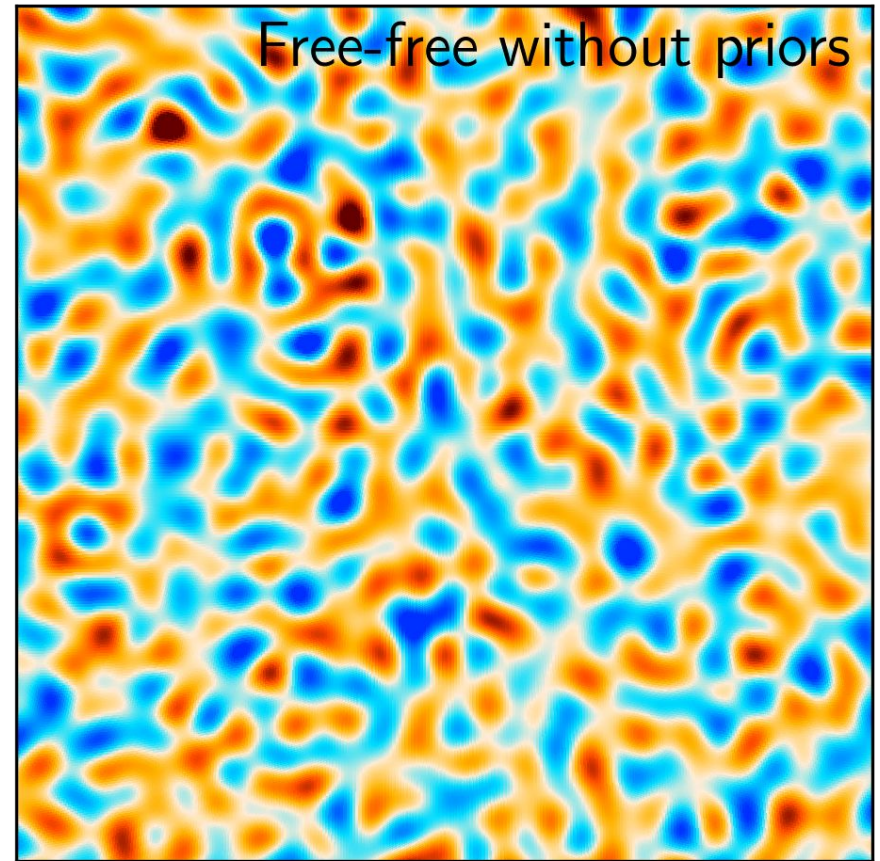
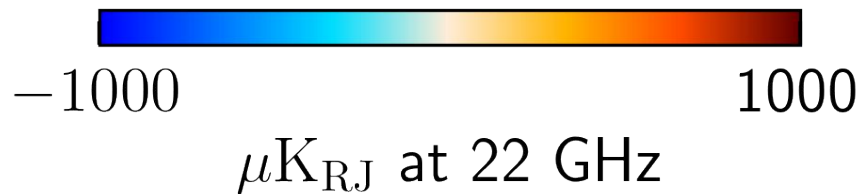
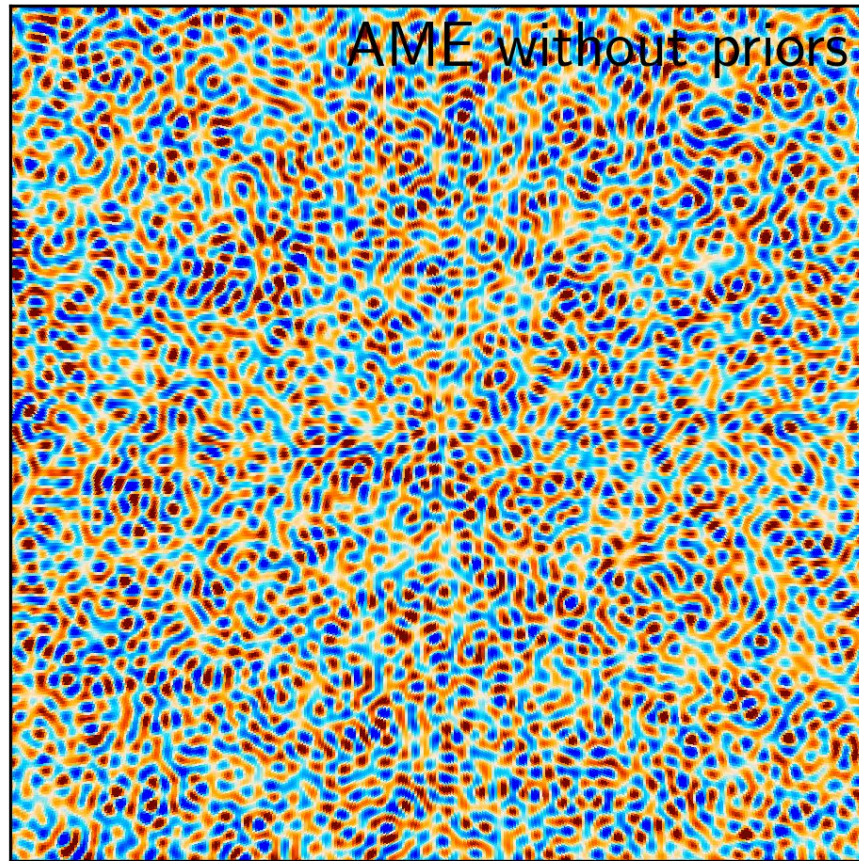
μK_{RJ} at 40 GHz



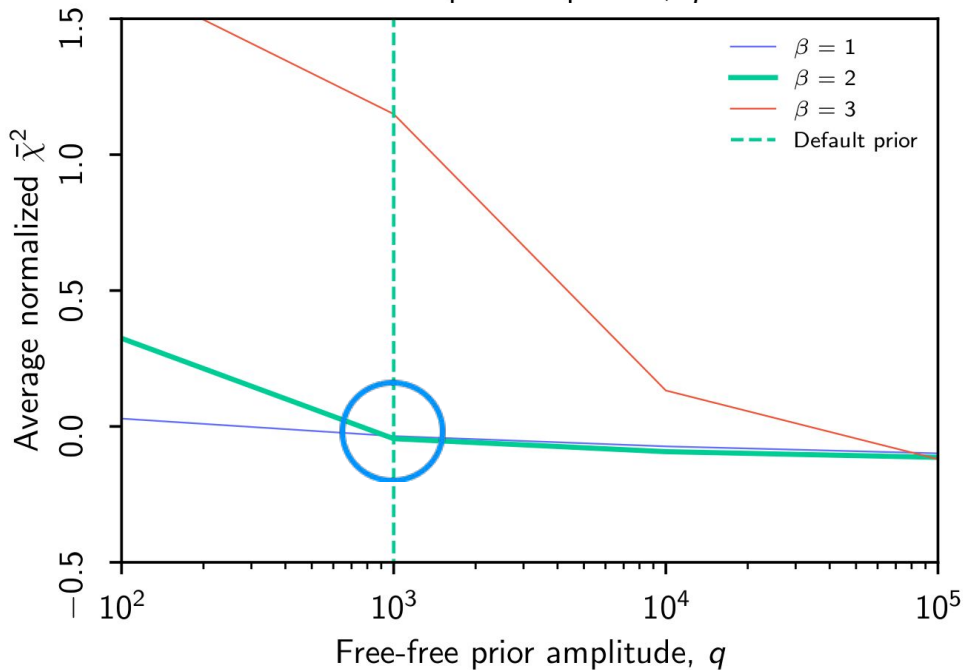
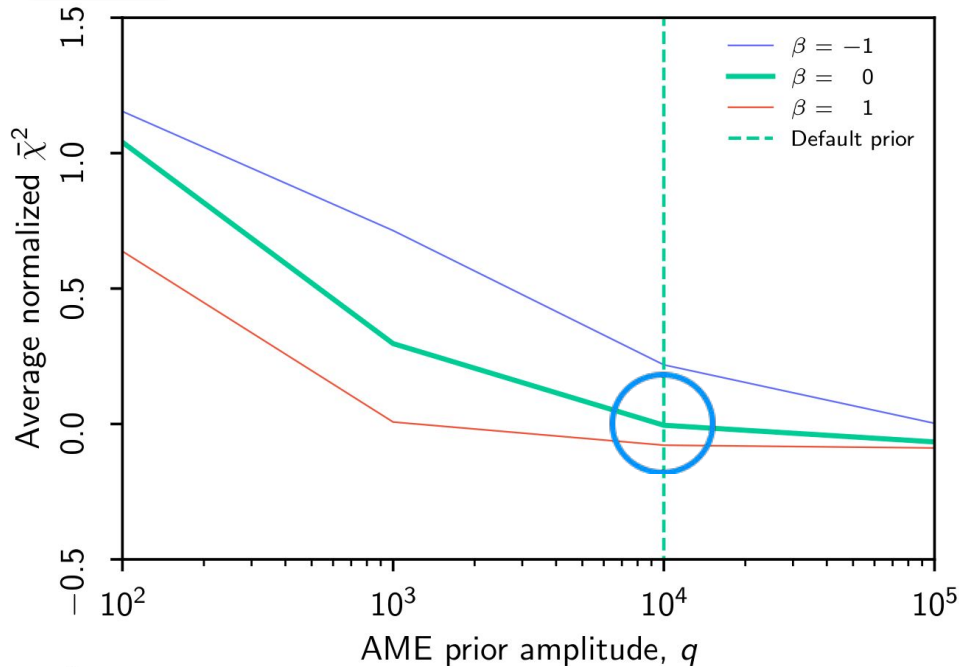
μK_{RJ} at 22 GHz

Amplitude degeneracies and priors

15' FWHM, $20^\circ \times 20^\circ$ centered on galactic south pole



Amplitude degeneracies and priors



Implement an amplitude prior with mean maps based on:

- *Planck* 2015 free-free map,
- scaled *Planck* 857 GHz,

The prior RMS is specified as

$$\hat{D}(\ell) = q \left(\frac{\ell}{\ell_0} \right)^\beta$$

q ~ prior amplitude

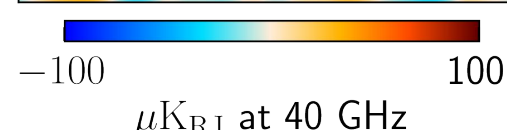
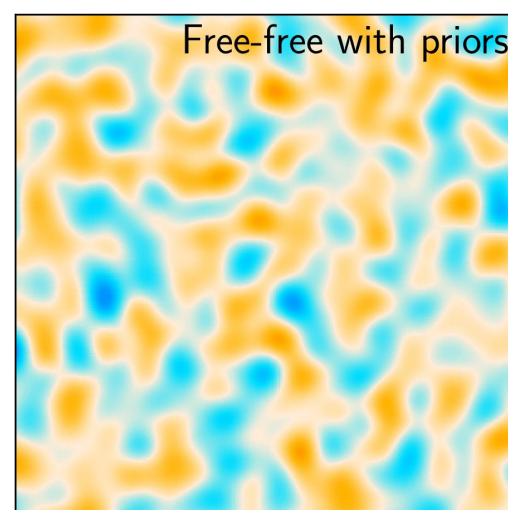
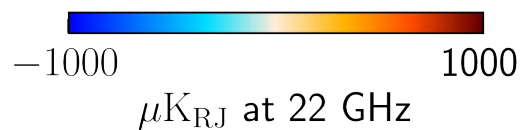
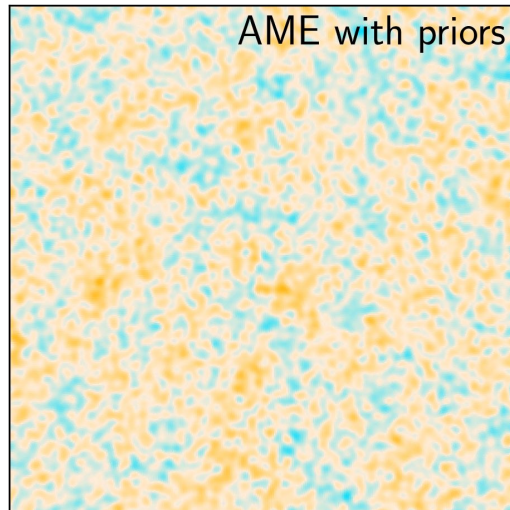
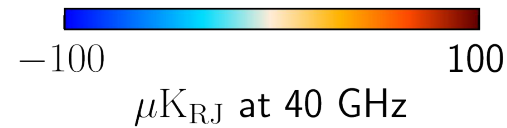
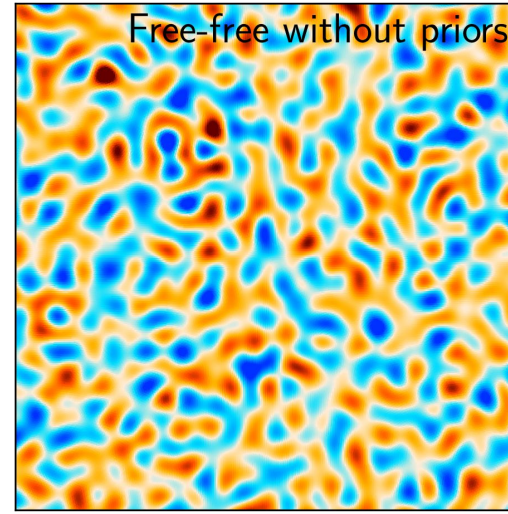
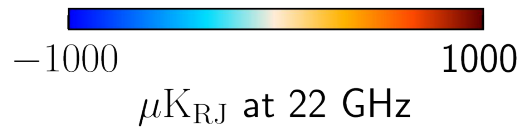
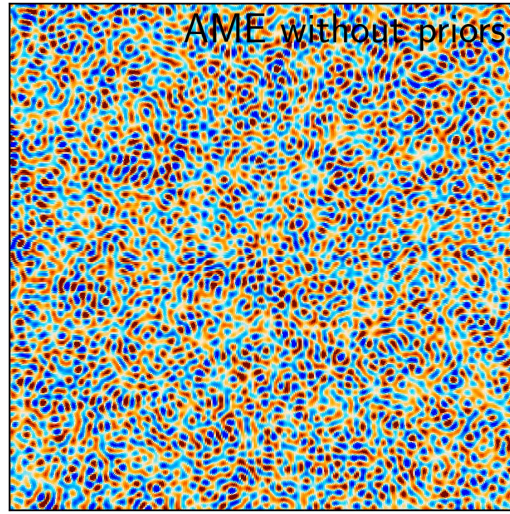
β ~ tilt parameter

ℓ_0 ~ pivot multipole = 50

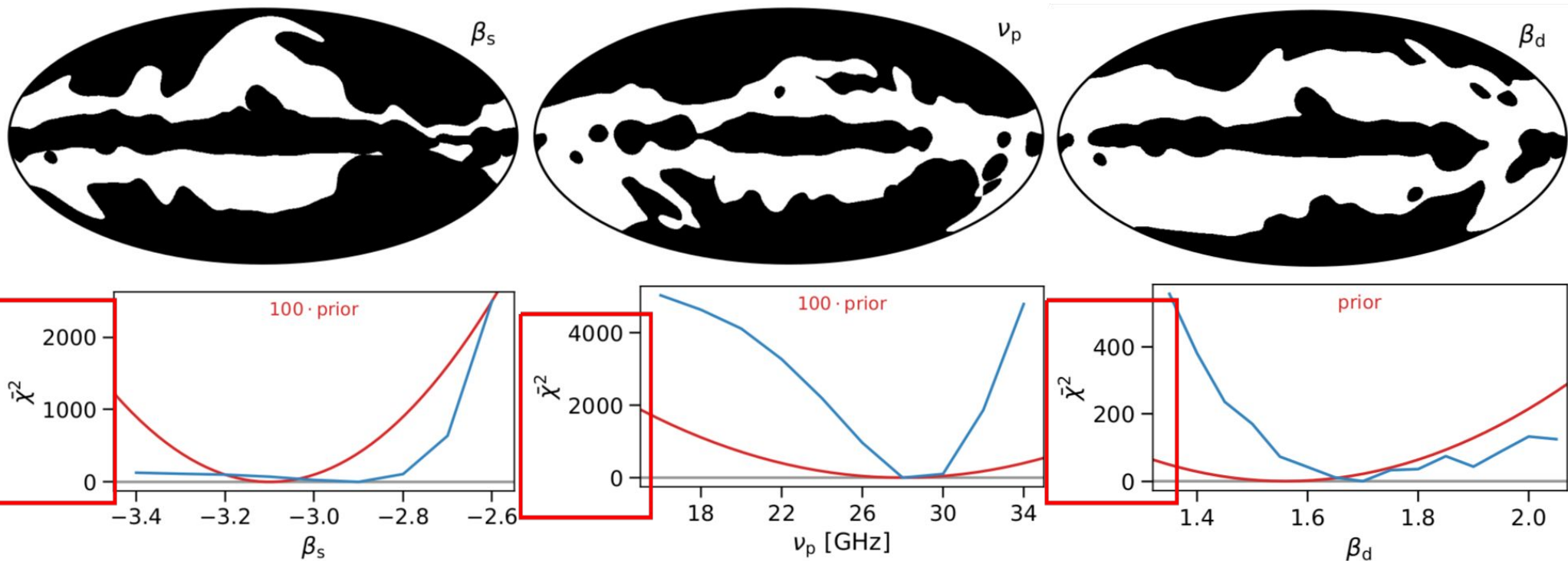
$$\bar{\chi}^2 = \frac{\chi^2 - \nu}{\sqrt{2\nu}}; \quad \nu = 15400$$

Amplitude degeneracies and priors

15' FWHM, $20^\circ \times 20^\circ$ centered on galactic south pole



Spectral parameter degeneracies and priors



Well constrained
by data.

Sample from data, with
Gaussian prior
 $N(-3.1, 0.1^2)$.
(Planck 2016, A&A, 594, A10)

Well constrained
by data.

Sample from data,
with Gaussian prior
 $N(28, 3^2)$ [GHz].

Prefers higher values,
diverges to > 2.0 when
sampled with other parameters

We only sample from
Gaussian prior $N(1.56, 0.03^2)$.
(Planck 2016, A&A, 594, A10)

$$\alpha_{\text{src}} = N(-0.1, 0.3^2)$$

Bennet et al. 2013, ApJS,
208, 20

$$T_e = 7000 \text{ K}$$

Planck 2016, A&A, 594, A10

$$T_{\text{dust}} = T_{\text{dust,HFI}}$$

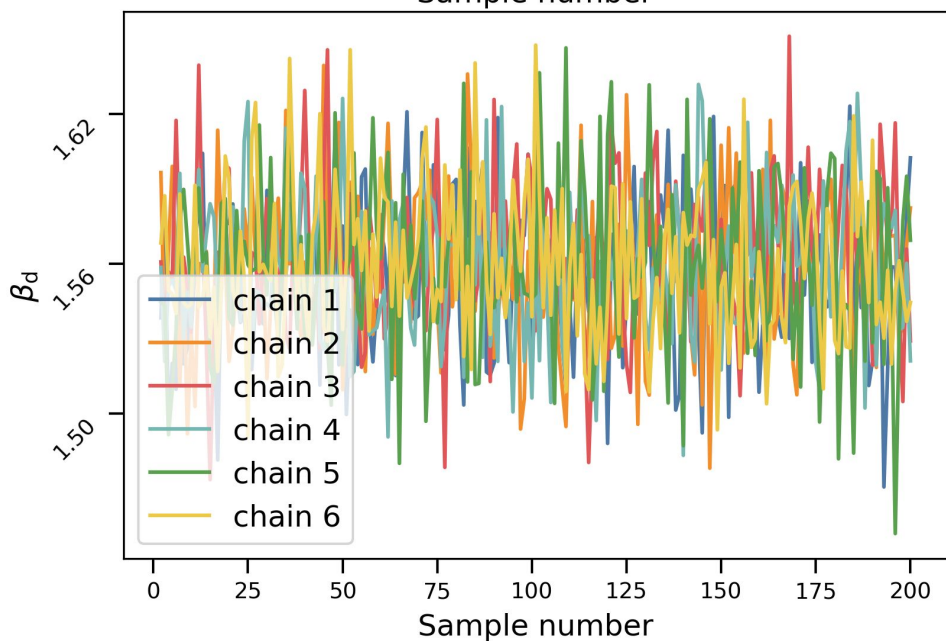
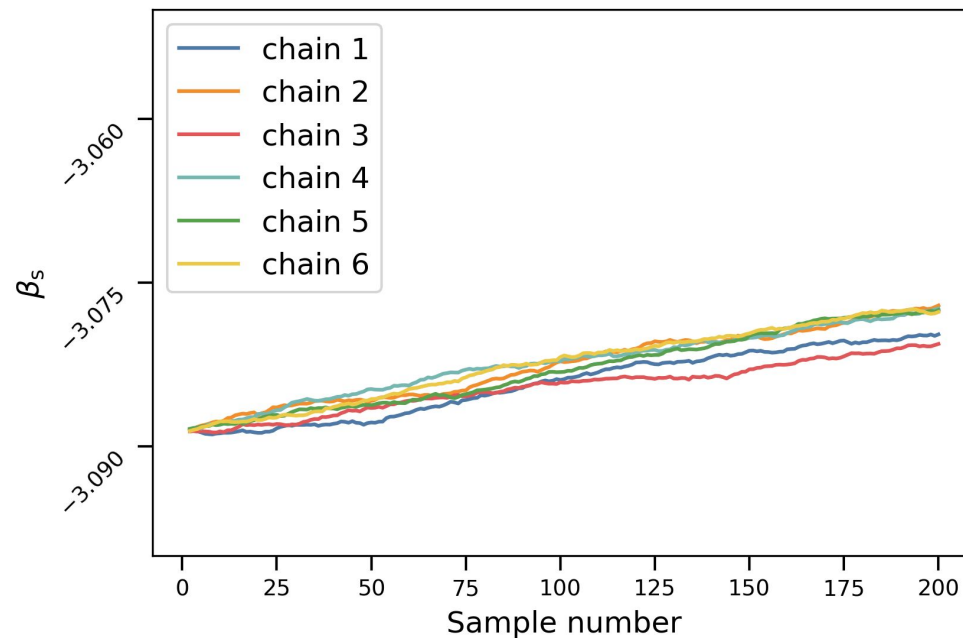
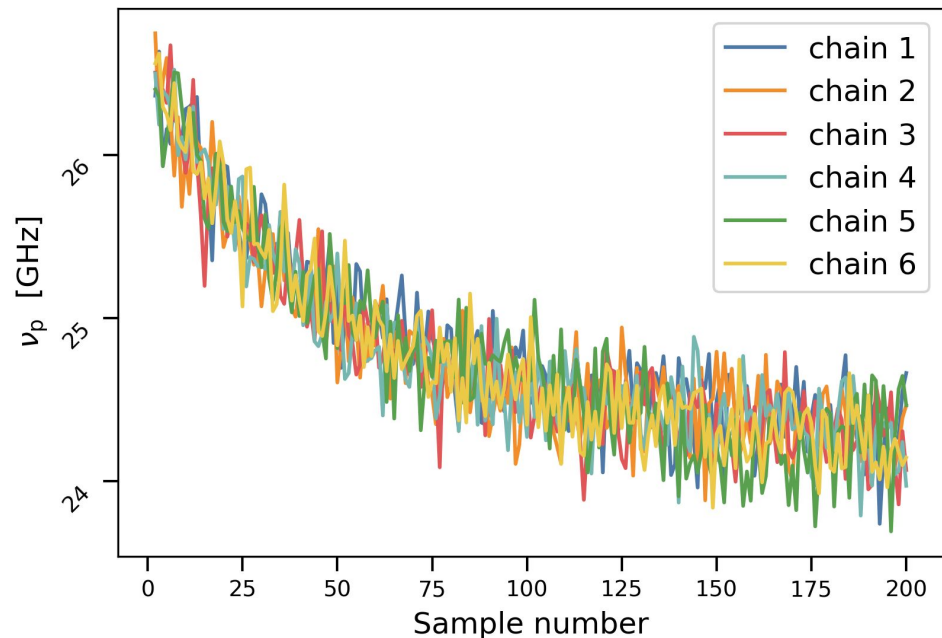
Planck Collaboration Int. LVII.
2020, A&A, in press
[arXiv:2007.04997]

Most recent *Planck* HFI



Results

Spectral parameters posteriors



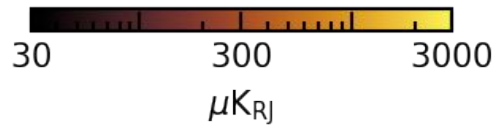
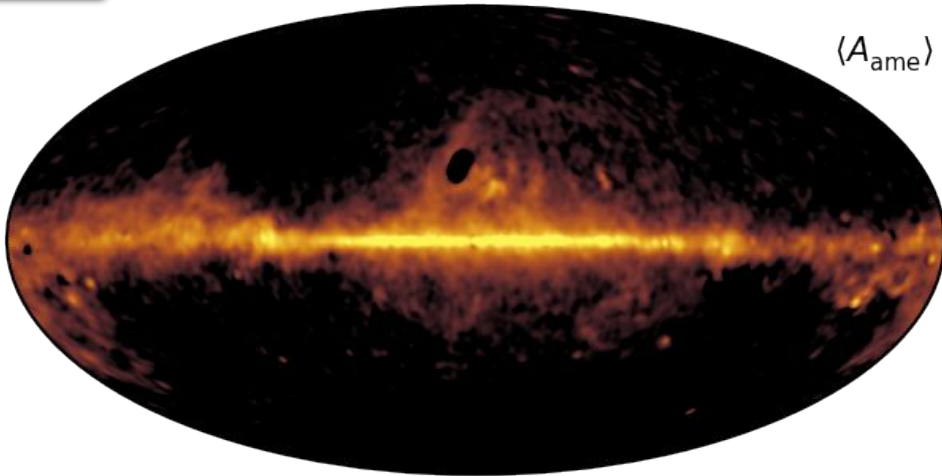
Parameter	Value	Sample range
ν_p	24.31 ± 0.21 GHz	150 – 200
β_s	-3.0819 ± 0.0025	50 – 200
β_d	1.559 ± 0.031	50 – 200

Low frequency amplitudes



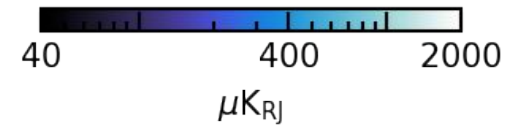
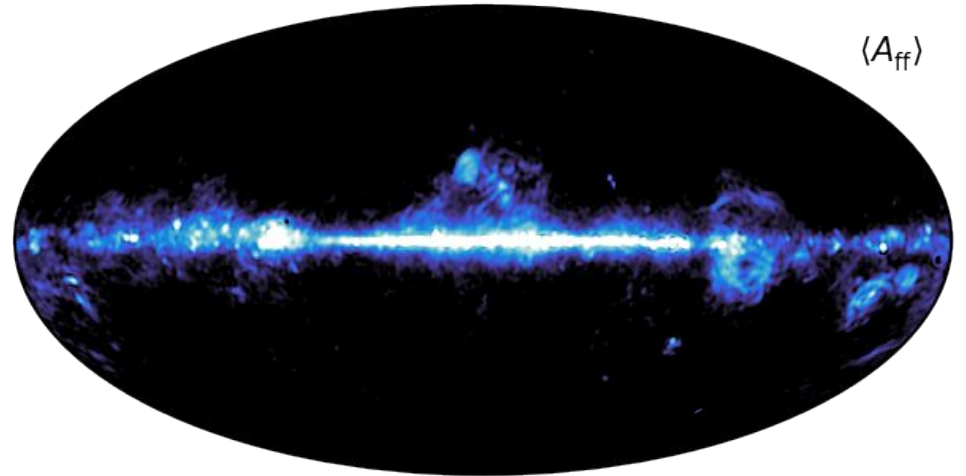
At 22 GHz

$\langle A_{\text{ame}} \rangle$



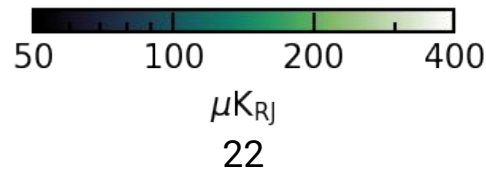
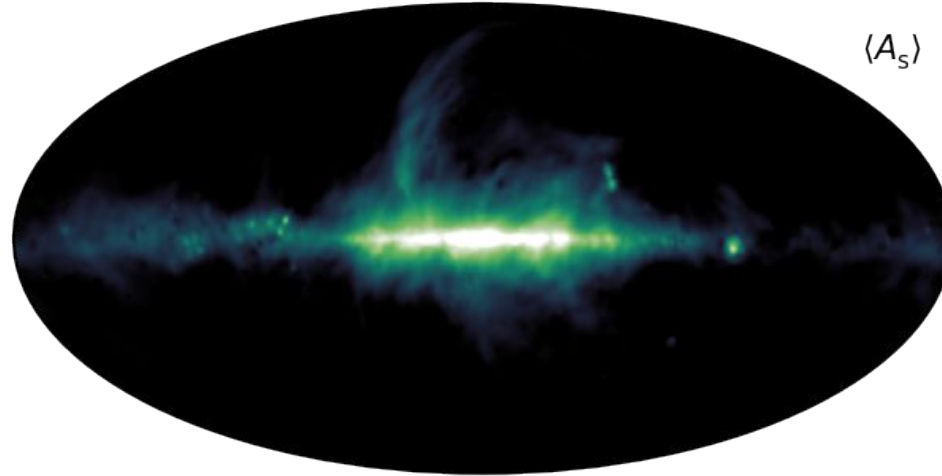
At 40 GHz

$\langle A_{\text{ff}} \rangle$



At 30 GHz

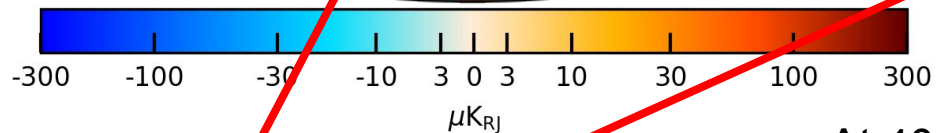
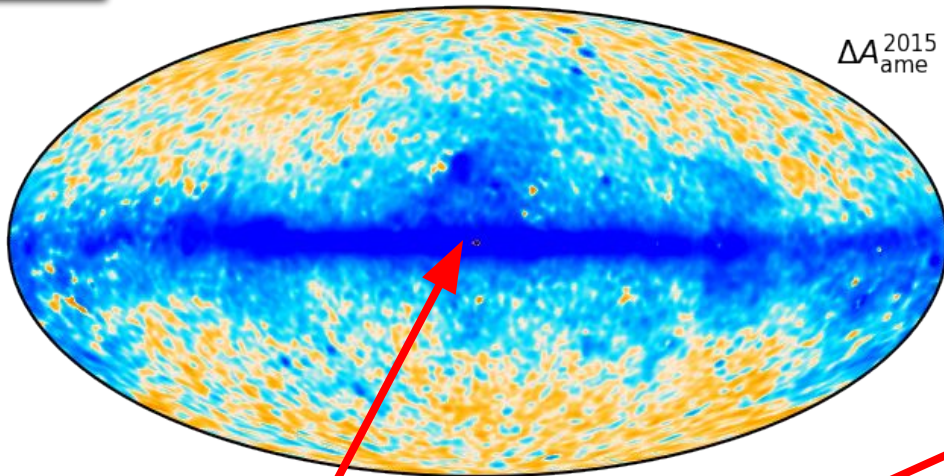
$\langle A_{\text{s}} \rangle$



Low frequency amplitude difference with *Planck* 2015

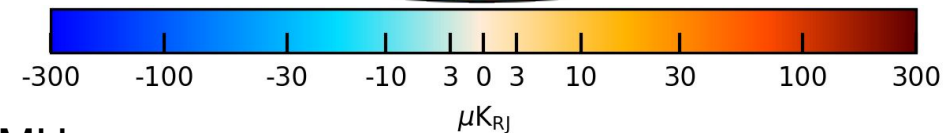
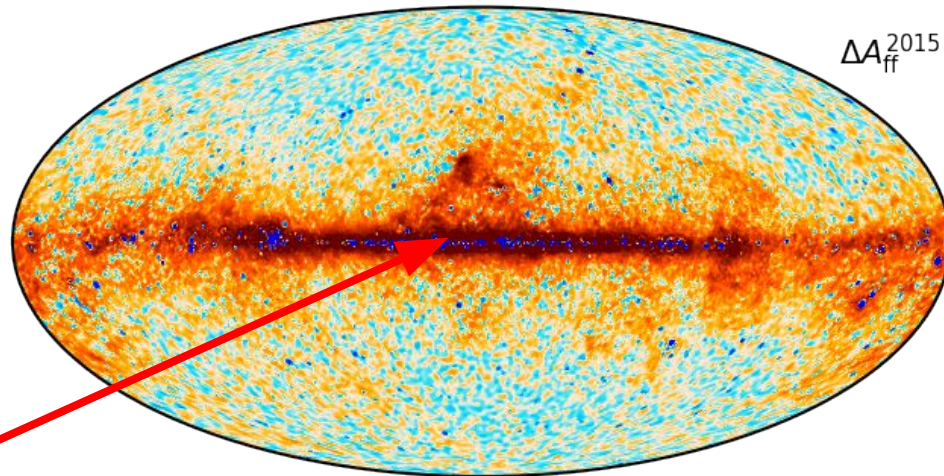
At 30 GHz

$\Delta A_{\text{ame}}^{2015}$



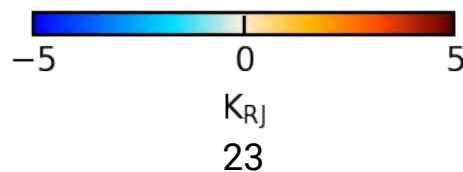
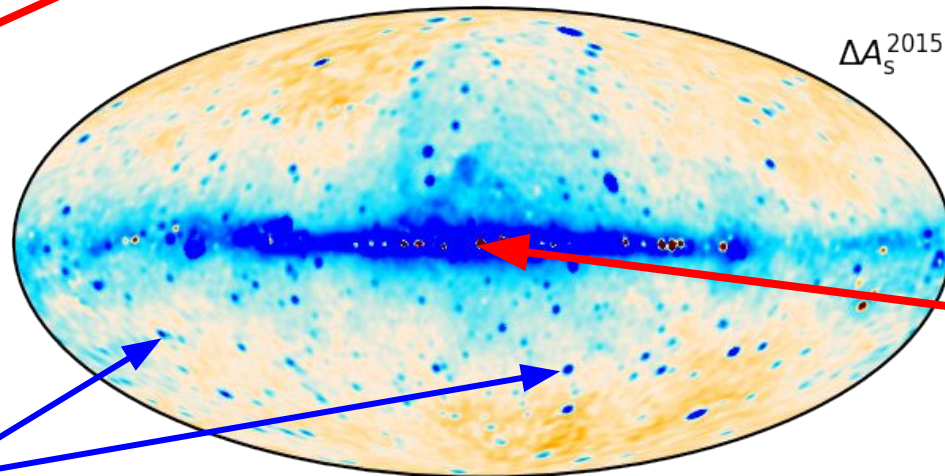
At 40 GHz

$\Delta A_{\text{ff}}^{2015}$



At 408 MHz

$\Delta A_{\text{s}}^{2015}$

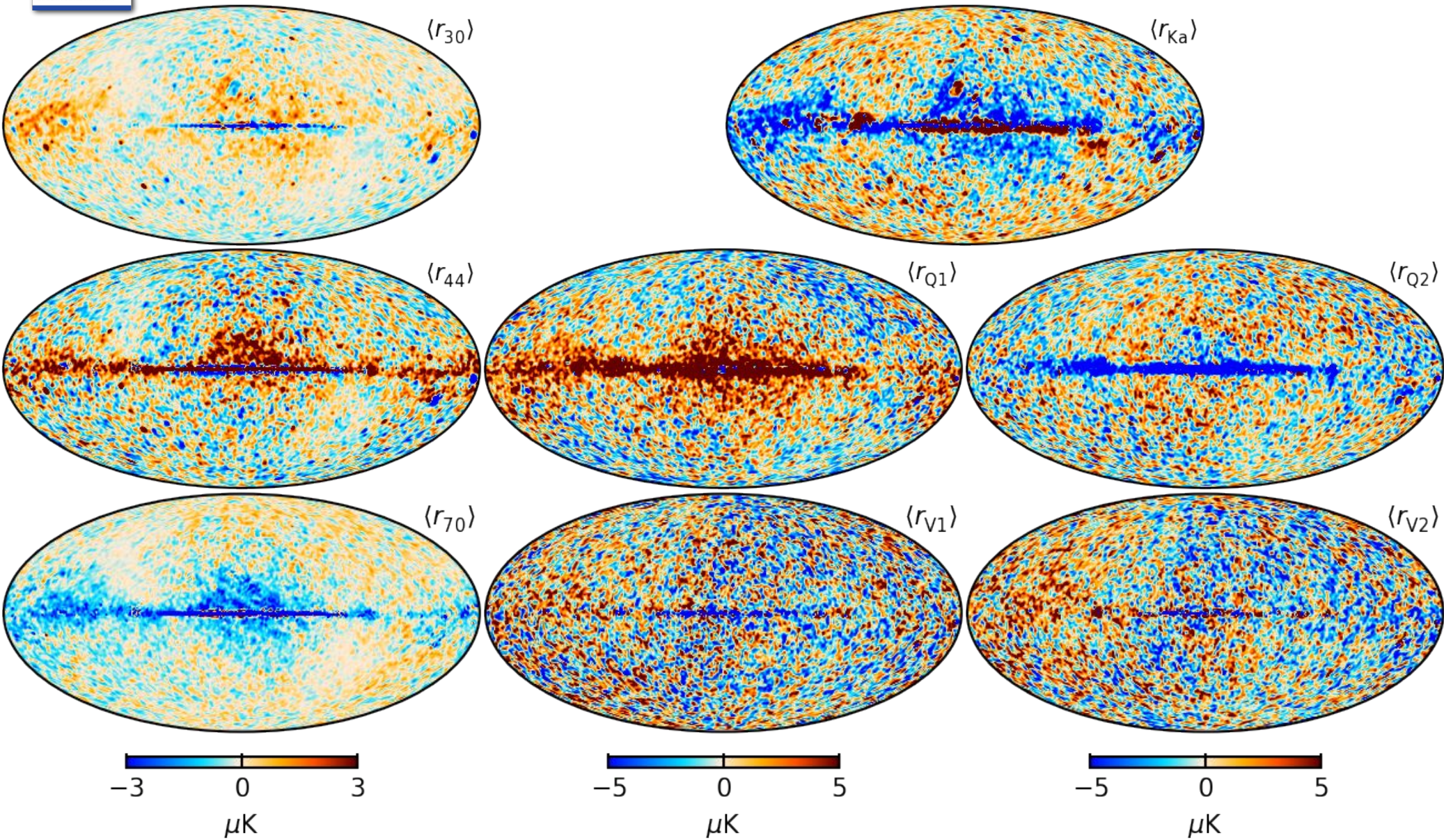


AME → Free-free
leakage

Point sources

Sign of spatial
variance in β_{s} ?
Consistent with
literature.

Goodness-of-fit: Residuals



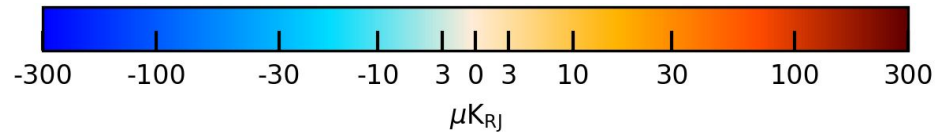
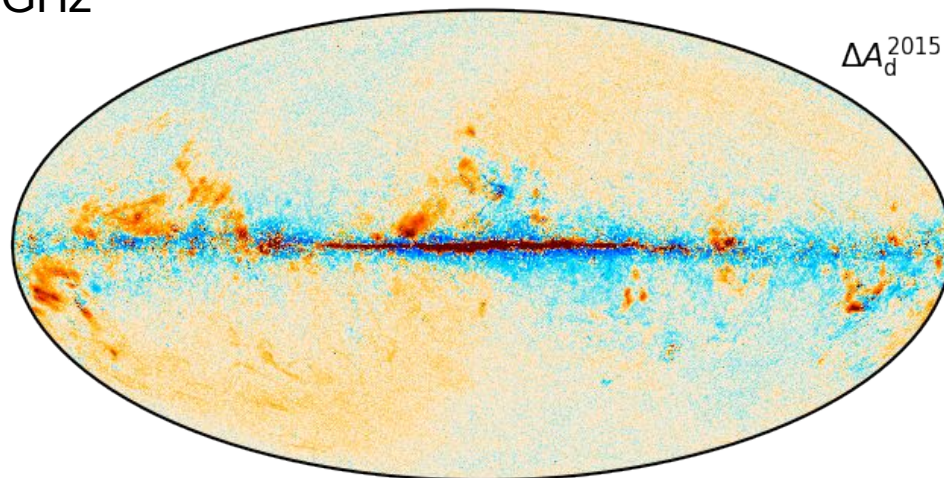
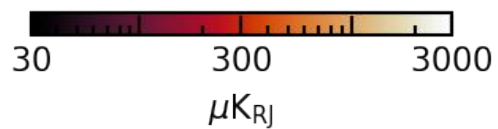
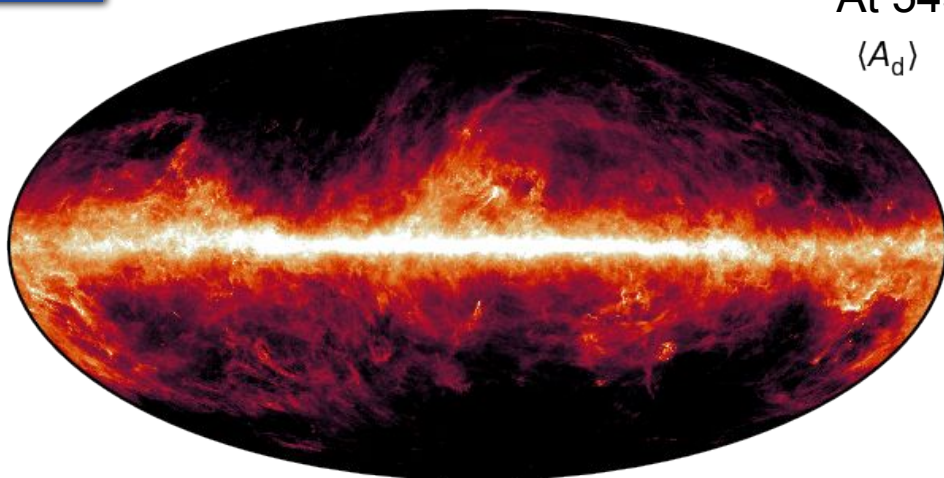
Thermal dust emission



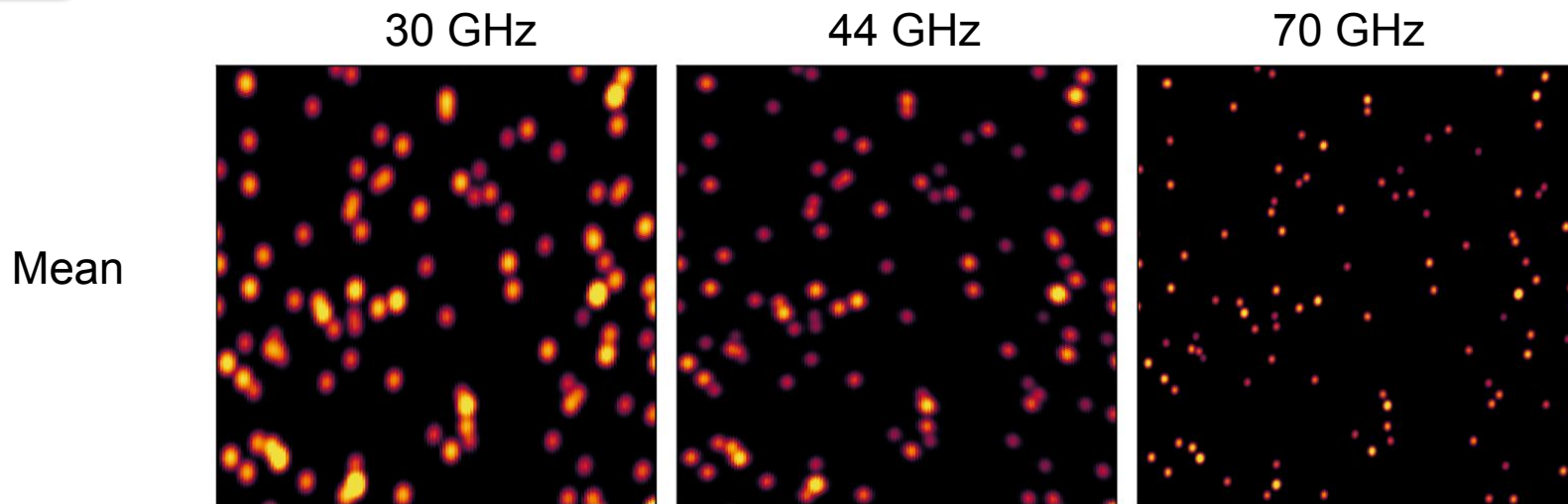
At 545 GHz

$\langle A_d \rangle$

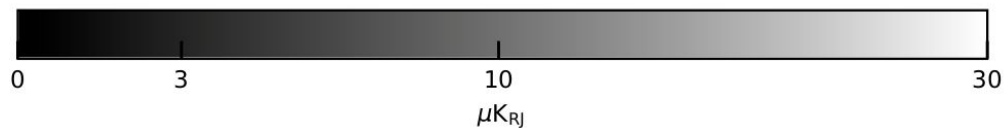
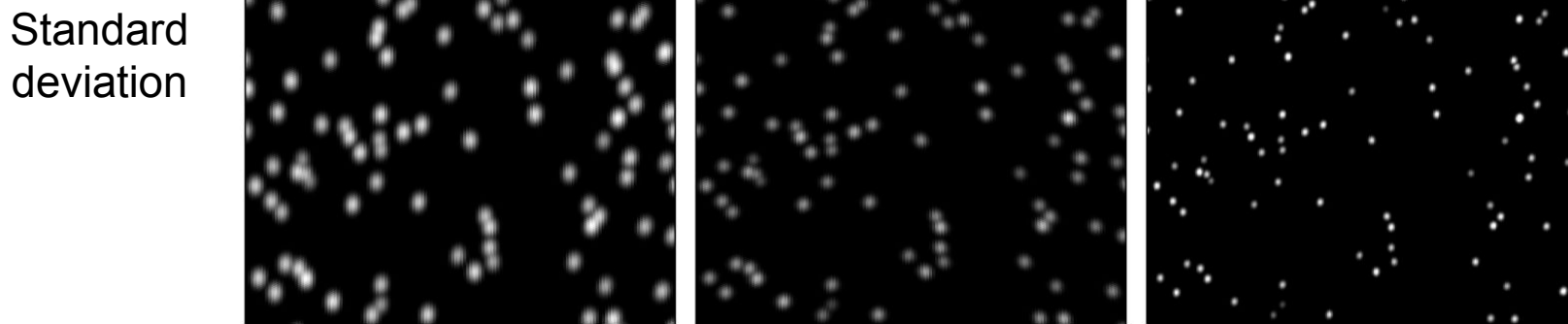
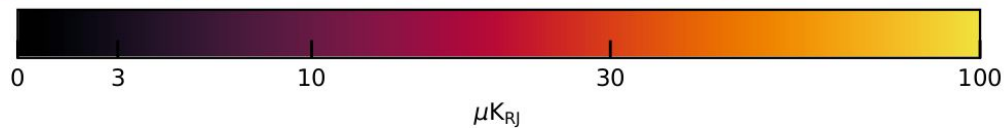
ΔA_d^{2015}



Compact sources

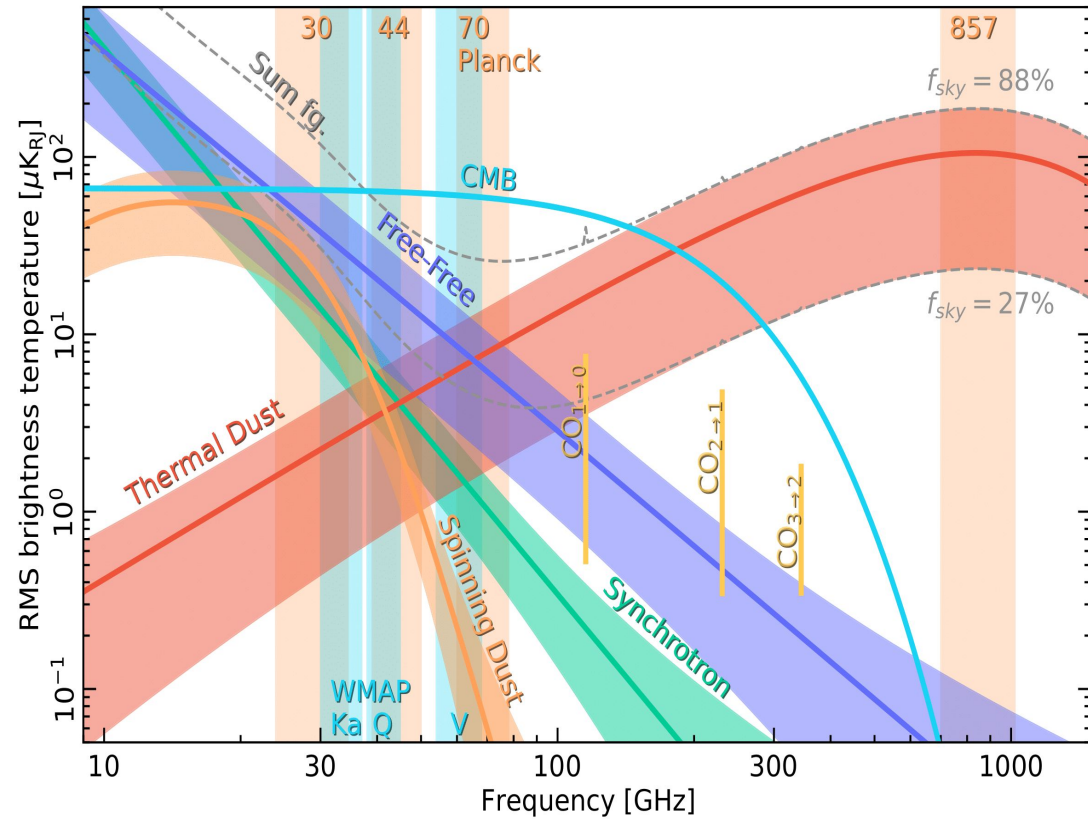


$20^\circ \times 20^\circ$
centered on
 $(l, b) = (90^\circ, 70^\circ)$



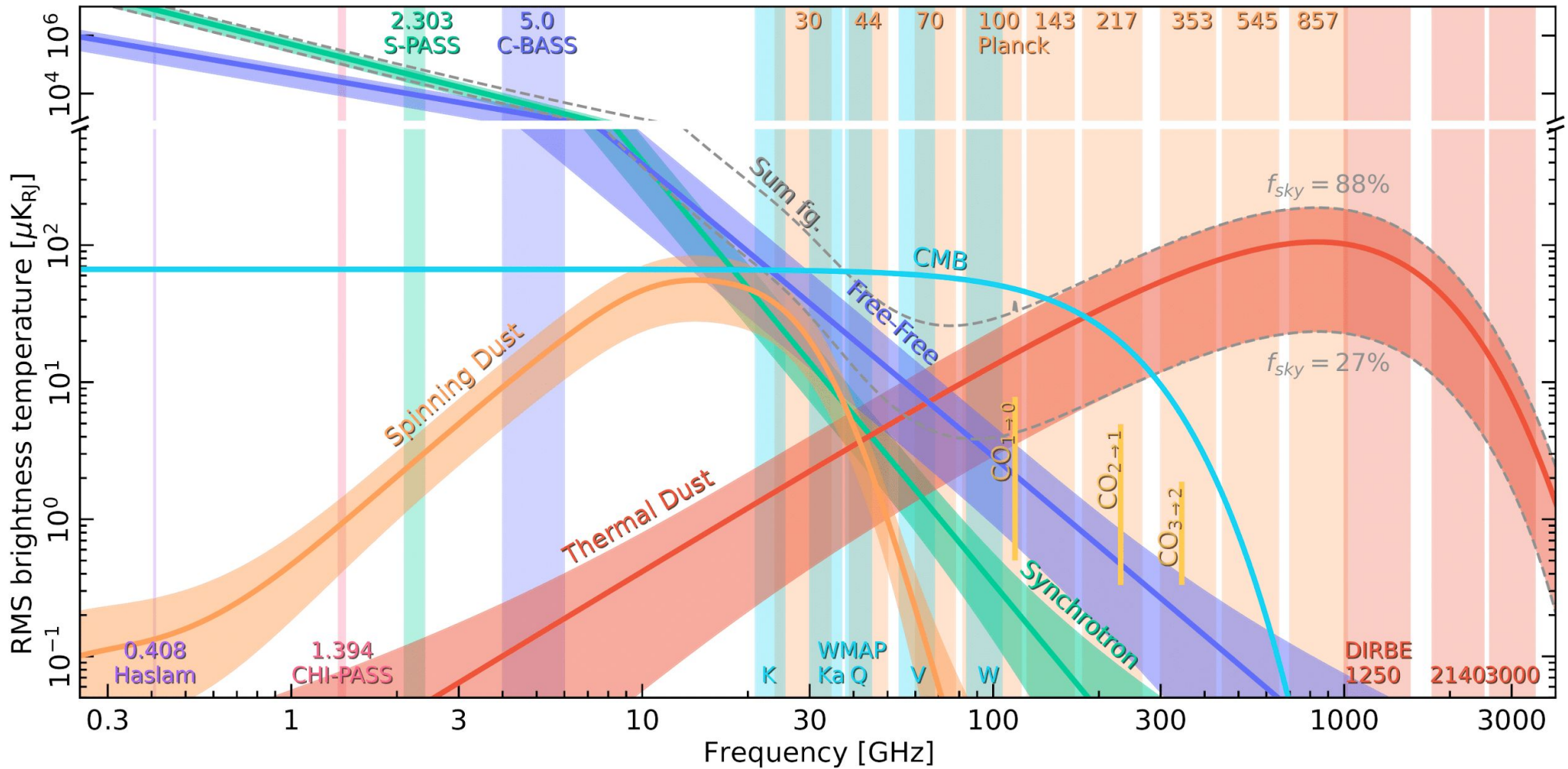
Haslam
0.408

0.408 GHz





Outlook



The Cosmoglobe project

- Marginal likelihood ⇒ faster sampling of correlated posteriors
 - Amplitude priors ⇒ reduce degeneracies; AME, free-free, CMB
 - Spectral parameter priors ⇒ constrain weakly determined parameters while still propagating uncertainties
-
- Degeneracies between AME, free-free, and synchrotron amplitudes
 - More datasets needed to break degeneracies.
 - Long burn-in for AME and synchrotron, optimize pivot frequencies?
-
- Next step: Populate with many more datasets (Planck HFI, S-PASS, C-BASS, CHI-PASS, DIRBE) to break degeneracies and constrain the full model. This is the main goal of `CosmoGlobe`!

This project has received funding from the European Union's Horizon 2020 research and innovation programme under grant agreement No 776282



- “*BeyondPlanck*”
 - COMPET-4 program
 - PI: Hans Kristian Eriksen
 - Grant no.: 776282
 - Period: Mar 2018 to Nov 2020

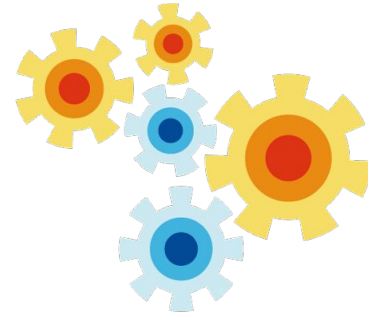
Collaborating projects:

- “*bits2cosmology*”
 - ERC Consolidator Grant
 - PI: Hans Kristian Eriksen
 - Grant no: 772 253
 - Period: April 2018 to March 2023
- “*Cosmoglobe*”
 - ERC Consolidator Grant
 - PI: Ingunn Wehus
 - Grant no: 819 478
 - Period: June 2019 to May 2024

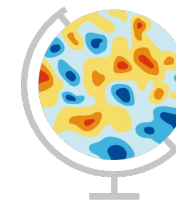


Questions?

Beyond PLANCK



Commander



Cosmoglobe Beyond PLANCK